International Journal of Power Electronics and Drive System (IJPEDS)
Vol. 7, No. 3, September 2016, pp. 835~853
ISSN: 2088-8694, DOI: 10.11591/ijpeds.v7.i3.pp835-853

Interleaved Boost Converter Fed with PV for Induction Motor/Agricultural Applications

A. Ramesh[1], M. Siva Kumar[2], O. Chandra Sekhar[3]
[1,3] KL University, Guntur, India
[2] Head of the Department, Gudlavalleru Engineering College, Gudlavalleru, AP, India

Article Info

Article history:

Received Nov 12, 2015
Revised Mar 2, 2016
Accepted Apr 3, 2016

Keyword:

Agriculture
Boost converter
Induction motor
Inter leaved boost converter
PV system

ABSTRACT

In present Electricity market Renewable Energy Sources (RES) are gaining much importance. The most common Renewable Energy Sources are Photo voltaic (PV), fuel cell (FC) and wind energy systems, out of these three PV systems PV system can implemented in most of the locations. Due to the power cuts and power disturbances in Distribution systems agriculture application is concentrated on PV based Energy system. The use of PV system is increasing day by day in agriculture application, due to their ease of control and flexibility. PV Electrification schemes also involves various subsidies in government national and international donors. Especially in Agriculture field by use of PV one can achieve higher subsidy. The output of PV system is low voltage DC to have high efficiency. The motors used in agriculture field are Induction Motors (IM) fed from Three phase AC supply, to boost the PV output we need a high voltage gain boost converter along with PWM inverter to Induction motor drive. Out of various DC-DC converter configurations interleaved boost converter is gaining much attention, due to its reduction in size and Electromagnetic Interference (EMI). In this work we are proposing a PV fed interleaved boost converter with PWM inverter for agriculture applications. The design process of interleaved boost converter is explain detail and compared with existing boost converter. A 10 KW Power rating is choosing for the Induction motor drive and design calculations are carried out. A MATLAB/SIMULINK based model is developed for boost and interleaved boost converter and simulation results are presented, finally a scaled down hardware circuit design for interleaved boost converter and results are presented.

Corresponding Author:

A. Ramesh,
Department of Electrical and Electronics Engineering,
KL University, Guntur, India.
Email: ramesh_153@aec.edu.in

1. INTRODUCTION

PV systems are gaining high importance in rural electrification around the world, especially solar home systems and agriculture fields with continuous decrease of price and decrease of PV systems. It is gaining more attention in various electrical applications, due to the power disturbances and uncertainty in power agriculture field is looking for alternate source of energy. Due to the subsidies given by the government PV system is gaining more importance in agriculture application. The agriculture motors are normally used induction motor types, because of its low cost and rugged construction. This motor is driven from three phase 440V AC supply. In order to have high efficiency PV array system designed for low voltage to integrate this low voltage PV panel with Induction motor we need a boost converter and inverter.

As the power rating of the motor increases the boost converter need to carry high currents, it causes high stress on switches. To eliminate this problem interleaved boost converter is proposed in the literature.

Due to rise in power densities, the powerful tool to maintain input currents manageable with high efficiency is interleaved boost converter, still maintaining good power densities [1]. The advantages of interleaved boost converter are low stress on switches lower inductor and capacitor ripples [11-13]. An interleaved boost converter which is magnetically coupled to a voltage doubler circuit, providing a voltage gain greater than that of traditional boost converter was discussed in [2]. An interleaved boost converter which is magnetically coupled to a voltage doubler circuit, providing a voltage gain greater than that of traditional boost converter was discussed in [3]. An interleaved boost dc-dc converter is a suitable candidate for current sharing and stepping up the voltage on bulk power application [4-9]. A basic boost converter converts a DC voltage to a higher DC voltage. Interleaving adds additional benefits such as reduced ripple currents in both the input and output circuits [10]. This paper is mainly focusing on design considerations of interleaved boost converter for driving a 10Kw induction motor for agriculture applications. The design calculations of various components is clearly described in continuous conduction mode (CCM). The output of the interleaved boost converter is fed to three phase three level Diode clamped inverter. The schematic diagram of the interleaved boost converter is fed with PV for agriculture applications shown in Figure 1.

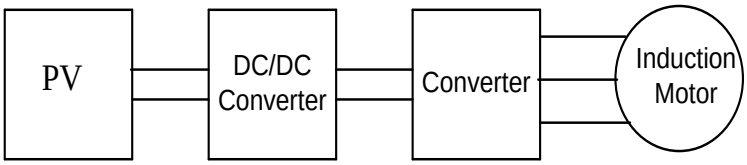

Figure 1. System Block Diagram

2. INTERLEAVED BOOST CONVERTER OPERATION

The schematic of the interleaved boost converter shown in Figure 2. The interleaved boost Converter consists of two boost converters connected in parallel controlled by phase-shifted switching function. The switching operation of the interleaved boost converter shown in Figure 3. In this application we have chosen only Dual interleaved boost converter, so the phase shift between each switch is 180^0. As the number of converters connected parallel increases the phase shift angle decreases.

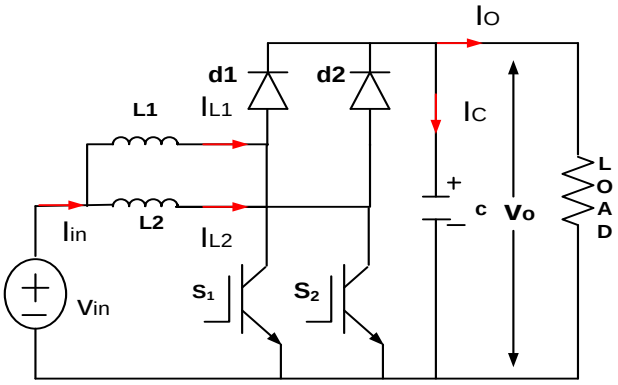

Figure 2. Interleaved Boost DC-DC Converter

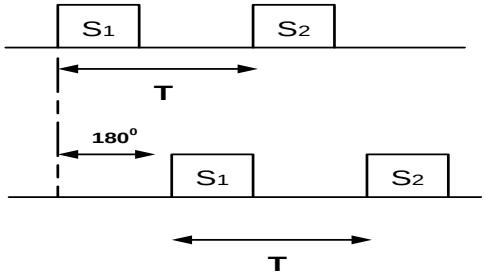

Figure 3. Timing diagram of Control Signal

The inductors L1 and L2 are having the same inductance value which is equivalent to L for simple calculations. Duty cycle of S1 was denoted by D1 like foe S2 as D2.The duty cycle values of both witches were equivalent to D. The operating mode of the converter can be explained as:

a. Stage I: Currents through inductor L1 starts to rise while being discharged through L2 when switch S1 is closed and S2 is opened at time T0.
b. Stage II: Currents through inductor L1 starts to discharge also being discharged through L2 through load when switch S1 and S2 are opened at time T1.

c. Stage III: Currents through inductor L2 starts to rise while being discharged through L1 when switch S2 is closed and S1 is opened at time T2.
d. Stage IV: Currents through inductor L1 starts to discharge also being discharged through L2 through load when switch S1 and S2 are opened at time T3 same as like in mode II. The cycle then repeats.

3. INDUCTION MOTOR

The induction motor is well-known for its simple and robust construction. Its low cost has found very wide range of industrial applications. A DC motor uses commutator and there is a problem of occurring sparks, due to this reason this DC motor cannot be used in polluted environments. Whereas an induction motor doesn't consists of any commutators and can be used in versatile environments. These advantages makes induction motor to made used in speed regulated industrial drive systems. Also there exists some technical problems while using induction motor drive since it requires two stages of conversion (ac-dc and dc-ac) in V/F control scheme the speed. Here a Reversing Voltage topology in 5 level and 7 level electrical converter is enforced for induction motor load that has superior characteristics over ancient topologies in terms of needed elements as switches, voltage leveling, management necessities and responsibility. Here SPWM controller has less complexness.

3.1. Dynamic Modeling of Induction Motor

There are two sets of identical voltage profile windings out of total windings in an exceedingly typical four pole machine. These two sets of windings are connected in non-parallel as shown in Figure 4(a). For the proposed inverter these two identical voltage profile winding coils are disconnected, and therefore the obtainable four terminals are taken out, like shown with in the Figure 4 (b). Since these two windings are separated equally, stator resistance, stator inductance and therefore magnetizing inductance of every identical voltage profile windings are capable the 1/2 the normal induction motor shown in Figure 4 (a). The voltage equation for the mechanical device winding is given by common dc link.

$$V_{a1} - V_{a2} = \left(\frac{r_s}{2}\right) * i_{as} + \left(\frac{L_{ss}}{2}\right) * i_{as} - \left(\frac{1}{2}\right) * \left(\frac{L_m}{2}\right) * i_{bs} - \left(\frac{1}{2}\right) * \left(\frac{L_m}{2}\right) * i_{cs} \quad (1)$$

$$V_{a3} - V_{a4} = \left(\frac{r_s}{2}\right) * i_{as} + \left(\frac{L_{ss}}{2}\right) * i_{as} - \left(\frac{1}{2}\right) * \left(\frac{L_m}{2}\right) * i_{bs} - \left(\frac{1}{2}\right) * \left(\frac{L_m}{2}\right) * i_{cs} \quad (2)$$

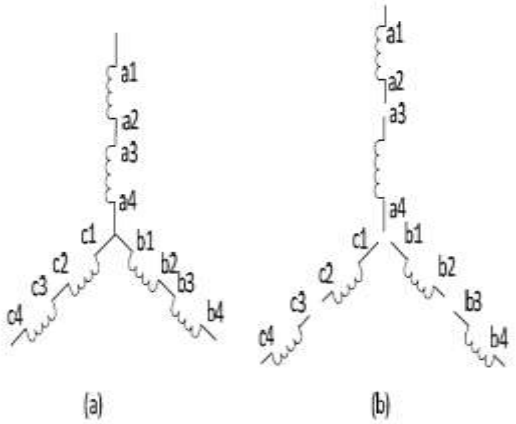

Figure 4. Stator winding of Induction Motor: (a) Basic arrangement (b) Arrangement for the proposed inverter

The effective voltage over the stator winding is the sum of the voltages over the two individual windings.

$$V_{as} = (V_{a1} - V_{a2}) + (V_{a3} - V_{a4}) \quad (3)$$

Phase voltage of the motor can be obtained by substituting equations (1) and (2) in (3)

$$V_{as} = r_s * L_{ss} + i_{as} * -\left(\frac{1}{2}\right) * L_m * i_{bs} - \left(\frac{1}{2}\right) * L_m * i_{cs} \quad (4)$$

In same way voltage equitation for the remaining phases are

$$V_{bs} = r_s * i_{bs} + L_{ss} * i_{bs} - \left(\frac{1}{2}\right) * L_m * i_{as} - \left(\frac{1}{2}\right) * L_m * i_{cs} \quad (5)$$

$$V_{cs} = r_s * i_{cs} + L_{ss} * i_{cs} - \left(\frac{1}{2}\right) * L_m * i_{as} - \left(\frac{1}{2}\right) * L_m * i_{bs} \quad (6)$$

Voltage equations in dq0 frame can be achieved from the general equations of induction motor.

$$V_{qs} = r_s * i_{qs} + \omega * \lambda_{ds} + \rho * \lambda_{qs} \quad (7)$$

$$V_{ds} = r_s * i_{ds} - \omega * \lambda_{qs} + \rho * \lambda_{ds} \quad (8)$$

$$V_{0s} = r_s * i_{0s} + \rho * \lambda_{0s} \quad (9)$$

$$V_{qr} = r_r * i_{qr} + (\omega - \omega_r) * \lambda_{dr} + \rho * \lambda_{qr} \quad (10)$$

$$V_{dr} = r_r * i_{dr} - (\omega - \omega_r) * \lambda_{qr} + \rho * \lambda_{dr} \quad (11)$$

$$V_{0r} = r_r * i_{0r} + \rho * \lambda_{0r} \quad (12)$$

Flux linkages are as follows

$$\lambda_{qs} = L_{ss} * i_{qs} + L_m * i_{qr} \quad (13)$$

$$\lambda_{ds} = L_{ss} * i_{ds} + L_m * i_{dr} \quad (14)$$

$$\lambda_{0s} = L_{1s} * i_{0s} \quad (15)$$

$$\lambda_{qr} = L_{rr} * i_{qr} + L_m * i_{qs} \quad (16)$$

$$\lambda_{dr} = L_{rr} * i_{dr} + L_m * i_{ds} \quad (17)$$

$$\lambda_{0r} = L_{1r} * i_{0r} \quad (18)$$

The equation for the electromagnetic torque (T_e) in terms of dq0 axis currents is

$$T_e = \left(\frac{3}{2}\right) * \left(\frac{P}{2}\right) * L_M * (i_{qs} * i_{dr} + i_{ds} * i_{qr}) \quad (19)$$

Speed of rotor in terms of Torque is

$$\frac{d}{dt}\omega_e = \left(\frac{P}{2*J}\right) * (T_e - T_L) \quad (20)$$

where
d: direct-axis,
q: quadrature-axis,
s: stator variable,
r: rotor variable,
V_{qs}, $V_{ds,}$: stator voltages of q and d–axis,
V_{qr}, $V_{dr,}$: rotor voltages of q and d–axis,
r_r : resistance of rotor,
Vr_s : resistance of stator,
L_{1s}: leakage inductance of stator,
L_{1r}: leakage inductance of rotor,

I_{QS}, i_{ds}: stator currents of q and d–axis,
i_{qr}, i_{dr}: rotor currents of q and d–axis,
P: no. of poles,
J: moment of inertia,
Te: output electrical torque,
T_L: load torque.
Equations (1), (2) and (3) shows nothing difference between conventional induction motor and the motor shown in Figure 4 (b)

4. DESIGNING OF INTERLEAVED BOOST CONVERTER

Inter leaved boost converter, Mode 1: S1 ON, Mode 2: During S1 off & S2 ON as shown in Figure 5, Figure 5(a), and Figure 5(b). Figure 6 shown Operating Wavefor.

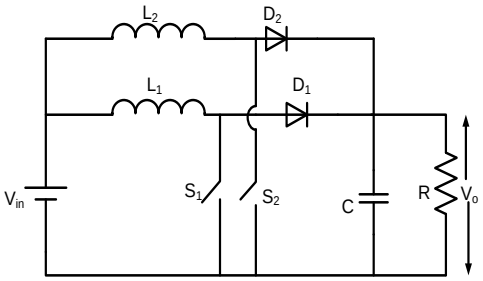

Figure 5. Inter leaved boost converter

Mode 1: S1 ON

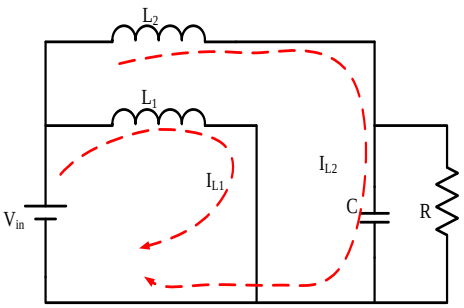

Figure 5(a). Mode 1: S1 ON

For inductor L_1

$$V_{in} = L_1 \frac{dI_1}{dt}$$

For inductor L_2

$$V_{in} - V_0 = L_2 \frac{dI_2}{dt}$$

Assume $\Delta I = I_2 - I_1$

$$V_{in} = L_1 \frac{\Delta I}{t_1}$$

$$t_1 = \frac{L \times \Delta I}{V_{in}} \quad (21)$$

Mode 2: During S1 off & S2 ON

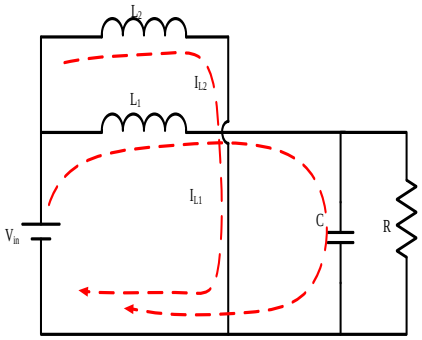

Figure 5(b). Mode 2: During S1 off & S2 ON

For inductor L_1

$$V_{in} - V_0 = -L_1 \frac{dI}{dt}$$
$$t_2 = \frac{\Delta I L_1}{V_0 - V_{in}} \quad (22)$$

Substitute t_1=DTs and t_2=(1-D)T_s

$$\Delta I = \frac{V_{in} \times t_1}{L}$$
$$\Delta I = \frac{V_0 - V_{in} \times t_2}{L}$$
$$\frac{V_{in} \times DT_s}{L} = \frac{(V_0 - V_{in})}{L}(1 - D)T_s$$
$$\frac{V_0}{V_{in}} = \frac{1}{1-D} \quad (23)$$

Total time period

$$T = t_1 + t_2 = \frac{\Delta IL}{V_{in}} + \frac{\Delta IL}{V_0 - V_{in}}$$
$$T = \frac{\Delta I L V_0}{V_{in}(V_0 - V_{in})} \quad (24)$$

Peak to peak ripple current

$$T = \frac{1}{f}$$
$$\Delta I = \frac{V_{in}(V_0 - V_{in})}{f L V_0} \quad (25)$$

$$\frac{\Delta I = V_{in} D}{f L} \quad (26)$$

Waveforms:

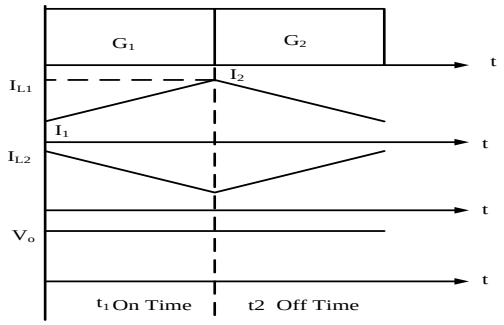

Figure 6. Operating Wavefor

For output capacitor

$$\Delta V_c = V_c - V_c(t=0) = \frac{1}{c}\int_0^{t_1} I_c\, dt$$
$$= \frac{It_1}{c}$$

Substitute

$$t_1 = \frac{(V_0 - V_{in}}{V_0 \times f}$$
$$\Delta V_c = \frac{I_0 K}{fc} \quad (27)$$

Condition for CCM operation. Take worst case ripple $\Delta I = 2I_L$

$$\Delta I = \frac{V_s K}{fL} = 2I_L = 2I_0 = 2 \times \frac{V_0}{R}$$

$$= \frac{2 \times V_{in}}{(1-K)R}$$

$$L_{critical} = \frac{K(1-K)R}{2f} \quad (28)$$

Take worst case ripple for capacitor

$$\Delta V_c = 2V_0$$

$$2V_0 = \frac{I_0 K}{fc} = 2I_0 R$$
$$C_{critical} = \frac{K}{2fR} \quad (29)$$

Specifications

P=10KW; V_0=400V;$I_0 = \frac{P}{V_0}$=$\frac{10\times10^3}{400} = 25A$

F=20 KHz; R=16Ω

$$\frac{V_0}{V_{in}} = \frac{1}{1-D} = \frac{400}{150} = \frac{8}{3}$$

$$1 - D = \frac{3}{8}$$

$$D = 1 - \frac{3}{8} = \frac{5}{8}$$

$$L_{critical} = \frac{(1-D) \times DR}{2f} = \frac{\left(1 - \frac{5}{8}\right) \times \frac{5}{8} \times 16}{2 \times 20 \times 10^3}$$

$$= \frac{15 \times 16}{16 \times 20 \times 10^3} = 0.75mH$$

In order to operate in CCM mode

$$L = 3 \times L_{critical} = 2.25mH$$

$$C_{critical} = \frac{D}{2fR} = \frac{5}{8 \times 2 \times 16 \times 20 \times 10^3}$$

$$= 0.9\mu F$$

In order to operate in CCM Mode we are choosing

$$C_{operate} = 200 \times C_{critical} = 10\mu F$$

Ripple current is

$$\Delta I = \frac{V_{ink}}{f \times L} = \frac{150 \times 5}{8 \times 20 \times 10^3 \times 2.25 \times 10^{-3}}$$
$$= 2\ A$$

Ripple Voltage is

$$\Delta V_c = \frac{I_0 \times K}{fc} = \frac{25 \times \frac{5}{8}}{20 \times 10^3 \times 200 \times 10^{-6}} = \frac{7.8}{2} = 3.9V$$

5. SIMULATION AND HARDWARE RESULTS

Table 1. Simulation Model Parameters

Input voltage	150V
Inductors	2.25mH
Capacitor	200μF
Resistance	16Ω
Duty ratio	62.5%
Stator resistance	2.8750 Ω
Stator inductance	8.5mH

5.1. Boost Converter

Figure 7 shows the simulation circuit of boost converter. A constant DC input source is applied as input to the converter circuit which steps up the voltage level at the output of the converter. In this boost converter only one switch is used to which gate pulses were applied through a pulse generator. Figure 8 shows the simulation result of the output current across the inductor. We can observe the presence of current ripple of 2 amperes. Figure 9 shows the gate pulse to the switch with a duty cycle of 62.5%. The simulation output result of voltage for a boost converter was shown in Figure 10 with zoomed result of the same shown

in Figure 11. We can observe there is a constant voltage at the output but in the zoomed result we can clearly observe that there is presence of ripple in the output voltage of the boost converter.

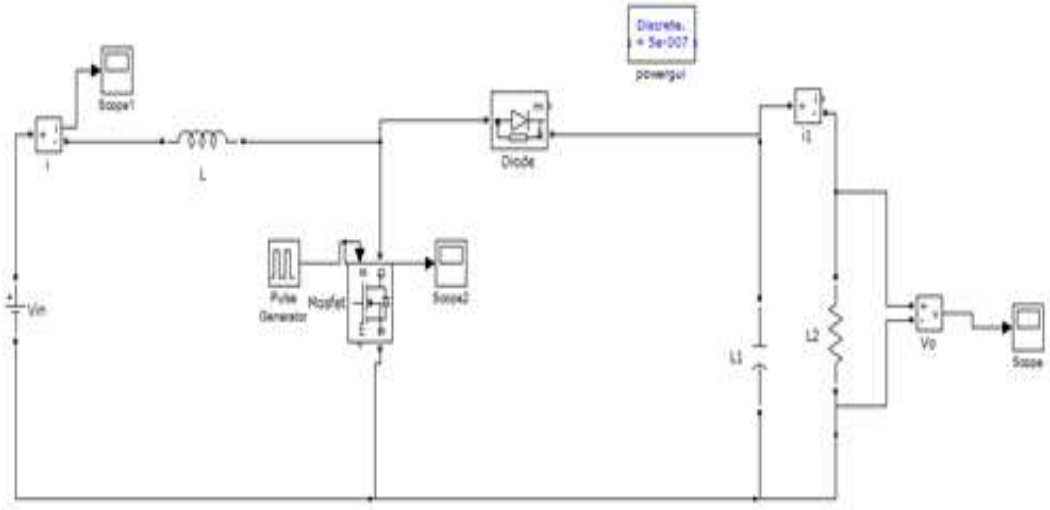

Figure 7. Boost Converter Simulation Model

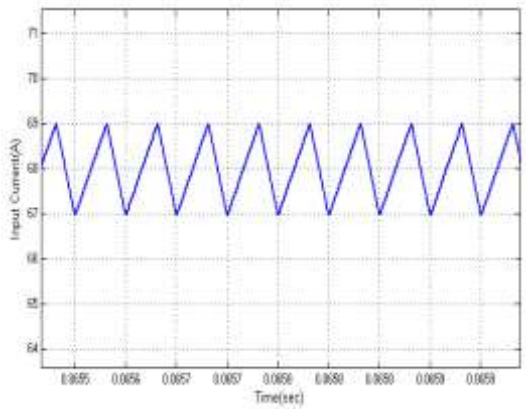

Figure 8. Simulation Results for Input Current and Inductor Current.

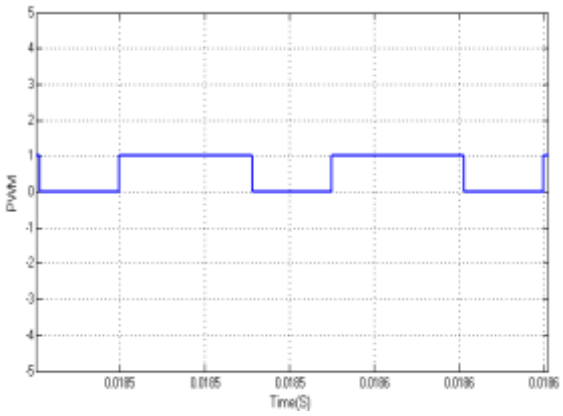

Figure 9. Simulation results for gating pulse

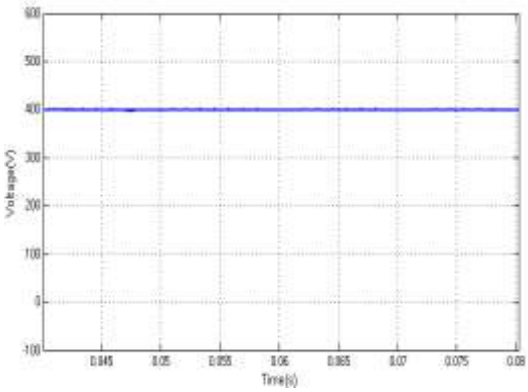

Figure 10. Simulation results for output voltage

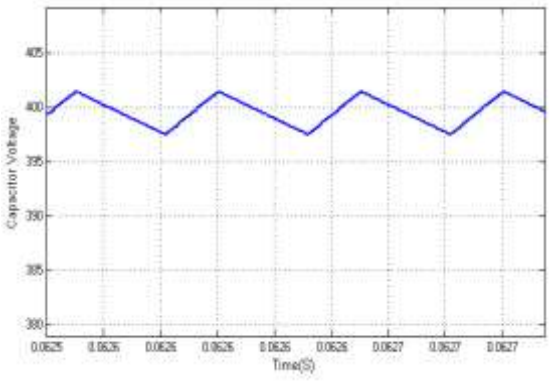

Figure 11. Simulation results for capacitor voltage

5.2. Interleaved Boost Converter

Figure 12 shown Interleaved Boost Converter Simulation Model. The output ripples in the boost converter can be reduced by using interleaved boost converter which employs two switches. Here the gate signals to the two switches are set by 180^0 apart each other. The simulation result of input current for interleaved boost converter is shown in Figure 13, we can observe there is a reduced ripple content in the input current when compared to normal boost converter. In normal boost converter we can see there is a 2A peak-peak ripple. But in interleaved boost converter the ripple content is confined to less than 1A peak-peak.

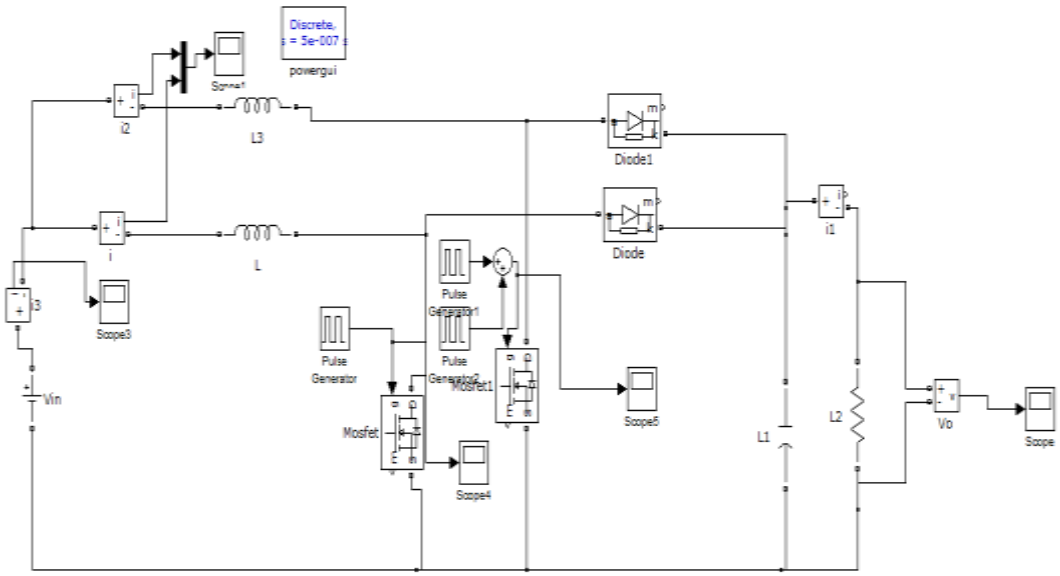

Figure 12. Interleaved Boost Converter Simulation Model

Figure 14 shows the input inductor currents which are having a phase shift of 180^0 obtained due to the application of pulses having the same 180^0 phase shift which are also shown in Figure 15 and Figure 16 for two switches. The result of output voltage for interleaved boost converter was shown in Figure 17. It appears to be there is no ripple content in the voltage at the output but the zoomed version shown in Figure 18 indicates that there is a ripple content in the output. But in the normal boost converter the ripples in the output voltage is high when compared to the ripple content in interleaved boost converter where the wave form fluctuates by just around 0.8Vp-p where in it around 5Vp-p in normal boost converter.

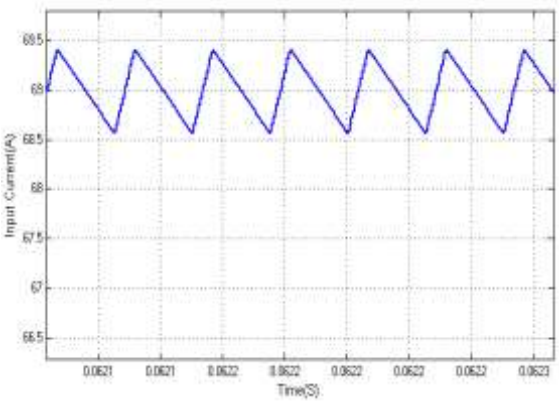

Figure 13. Simulation results for input current

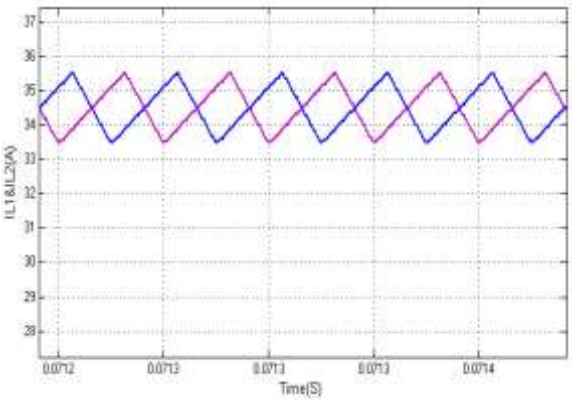

Figure 14. Simulation results for input inductor currents (IL1 and IL2)

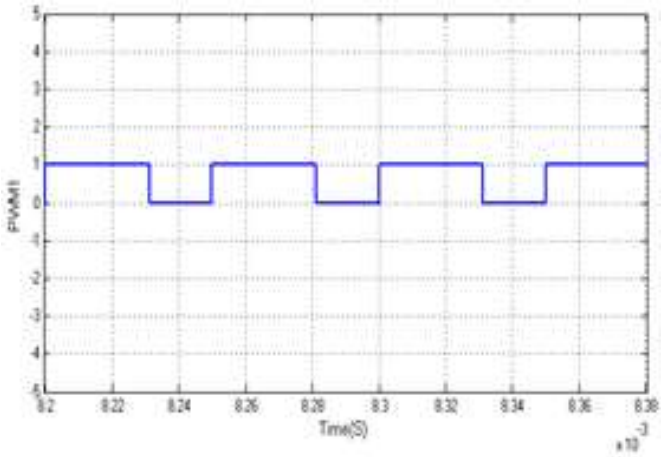

Figure 15. Simulation results for switch voltage S1

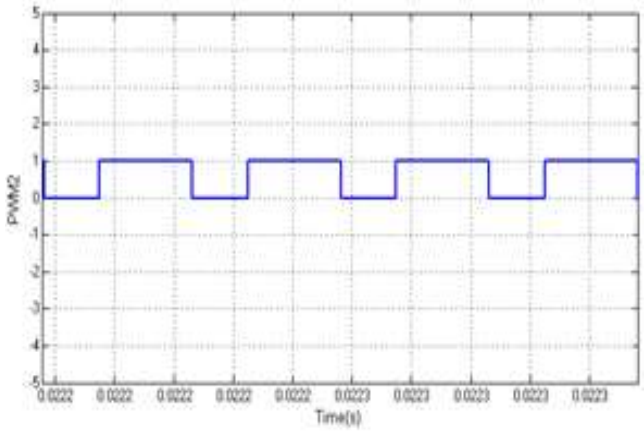

Figure 16. Simulation results for switch voltage S2

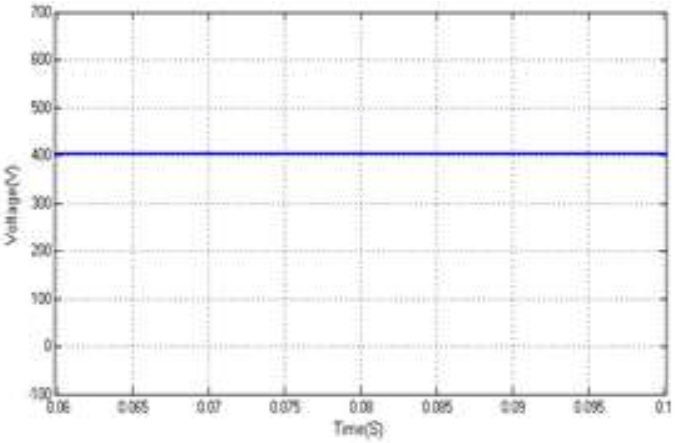

Figure 17. Simulation results for output voltage

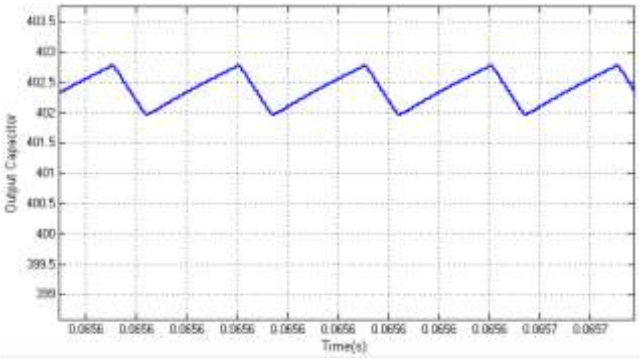

Figure 18. Simulation results for capacitor voltage

5.3. Interleaved Boost Converter with Induction Motor Drive

The discussed model for the cancellation of ripples interleaved boost converter is now applied to an induction motor drive to verify its performance characteristics. The Simulink model of interleaved boost converter for induction motor drive is shown in Figure 19. It consists of six switches, each driven by gate pulses. The output of the interleaved boost converter is fed to the induction motor through an inverter and its speed is controlled performing an induction motor drive operation.

Figure 20 shows the phase to phase voltages of inverter. The three phase voltages are shown separately and the line to line voltages of inverter are given in Figure 21. The stator current of induction motor along with the induction motor speed and torque are shown in Figure 22. The speed is obtained as 1470 rpm running with an asynchronous speed slip of 4%.

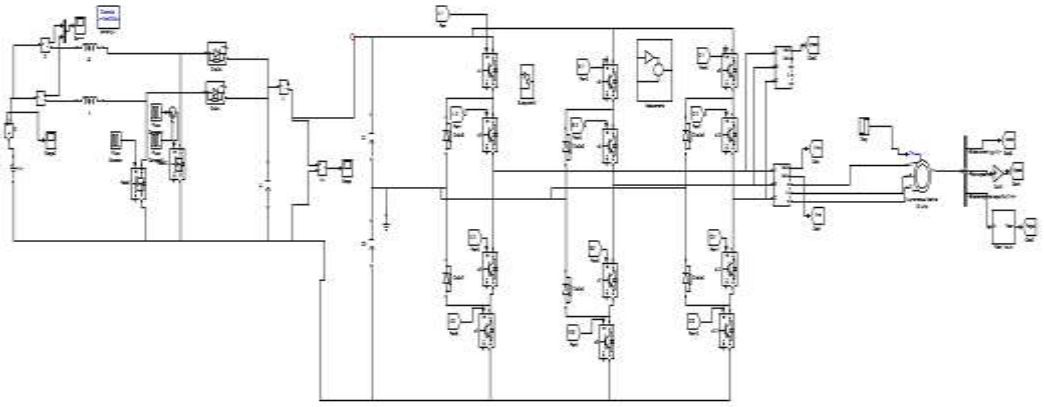

Figure 19. Interleaved Boost Converter Simulation Model with Induction Motor Drive

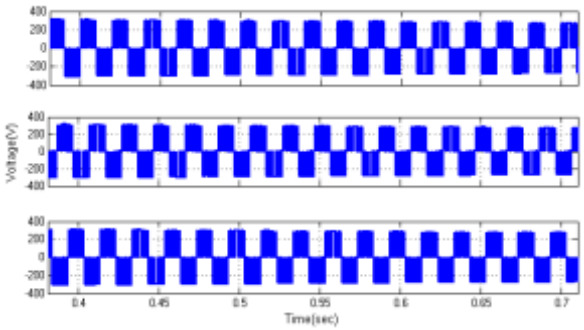

Figure 20. Inverter Phase to Phase Voltage

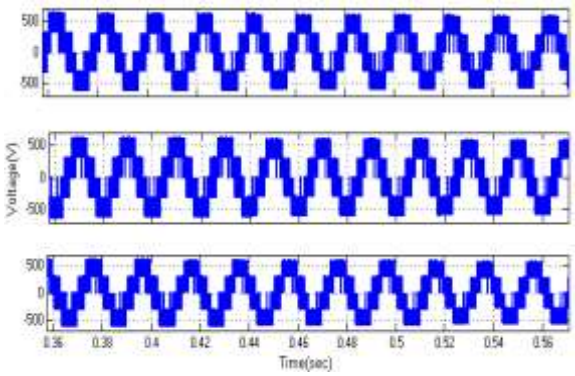

Figure 21. Inverter Line to Line Voltage

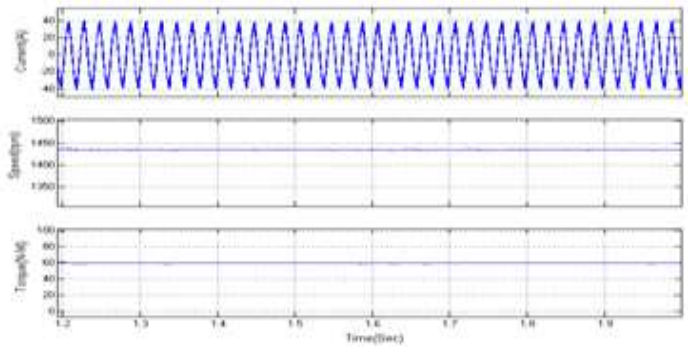

Figure 22. Stator Current, Speed and Torque of Induction Motor

Table 2. Hardware Parameters

MOSFET	IRF540n
Inductance used	1mH
Capacitance of Load	220uF
Diode	MUR1560

A small prototype for the above discussed interleaved boost converter is developed in hardware. Figure 23 shows the safety enhanced high step-up DC-DC converter for photovoltaic application and Figure 24 shows the control circuit based on SG3525 PWM controller IC. The input to the boost converter is 16V. The pulses for the MOSFET are generated using a PWM controller IC SG3525A, the prototype results were also shown.

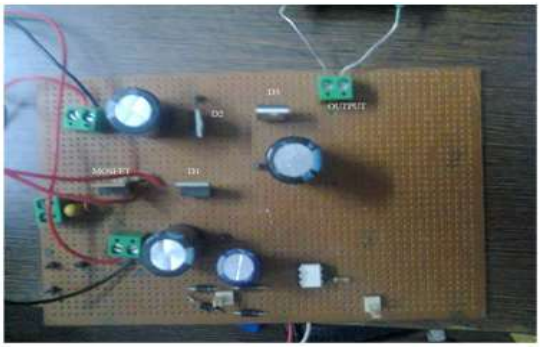

Figure 23. High step-up DC-DC Converter for Photovoltaic Application

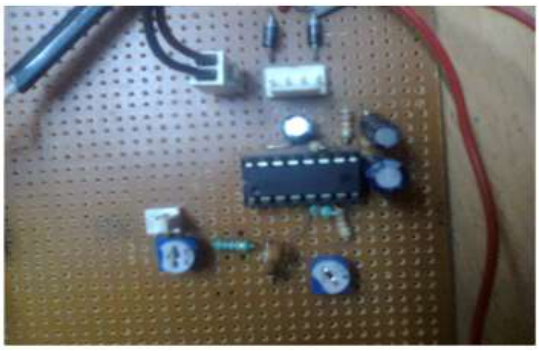

Figure 24. Control circuit based on SG3525 PWM controller IC

The prototype results of gate pulses for the two switches, switch 1 and switch 2 of interleaved boost converter are shown in Figure 25 and Figure 26 represents the prototype output result of the converter with 62.5% duty ratio. The SG3525A outputs are obtained as follows:

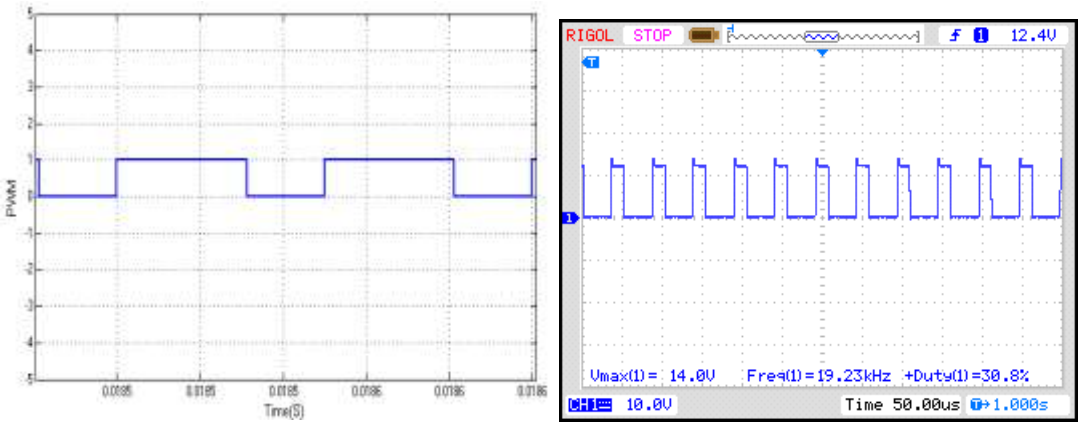

Switch 1

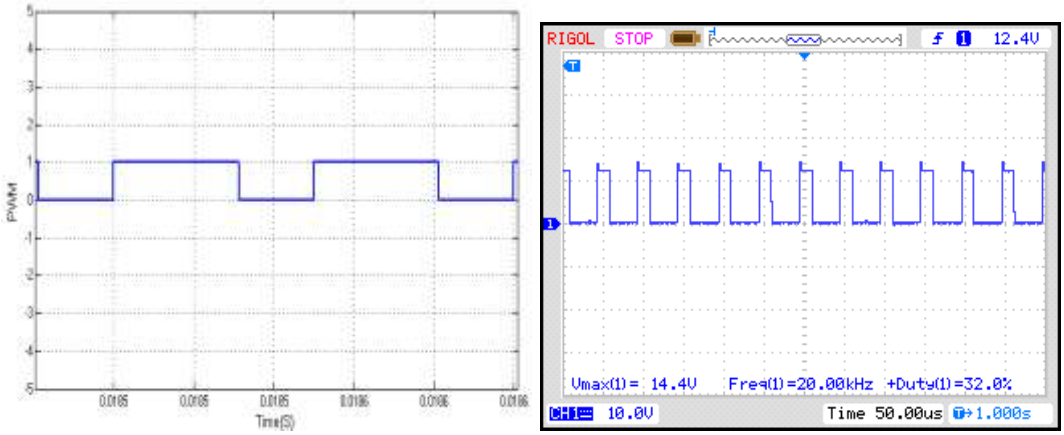

Switch 2

Figure 25. Comparision of hardware and simulink experimental results for Gate pulses for switch 1 and 2. The converter output at 62.5% duty ratio is obtained as:

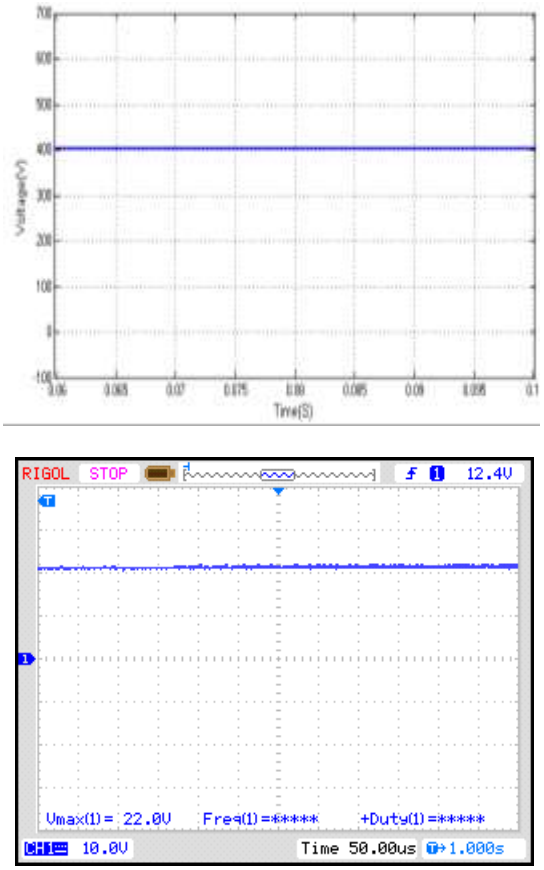

Figure 26. Scaled down hardware and software outputs of the converter

The prototype results of voltage across switch 1 and switch 2 were shown in Figure 27 and Figure 28 respectively and we can observe that the gate signals are having 180^0 phase shift between them. The voltage across diodes D1 and D2 are shown in Figure 29 and Figure 30 respectively. The prototype result of voltage across inductor is shown in Figure 31. The prototype results reflect the practical implementation of induction motor drive using interleaved boost converter for cancellation of ripple contents. The voltage waveforms across different components are obtained as follows:

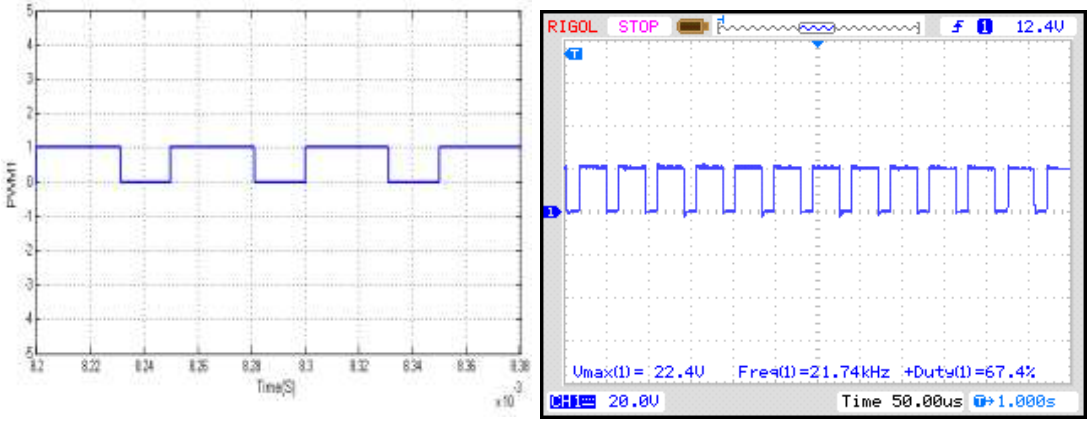

Figure 27. Comparitive Hardware and Simulink Results of Voltages Across Switch 1

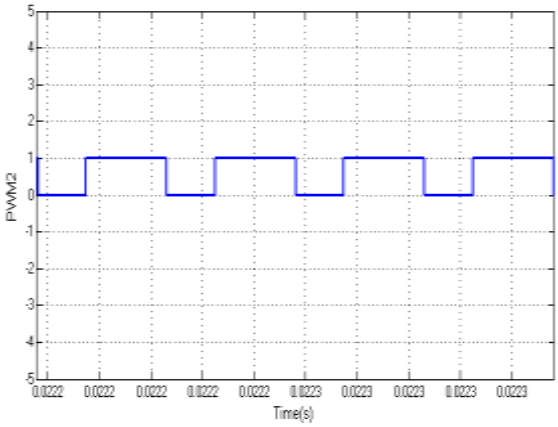

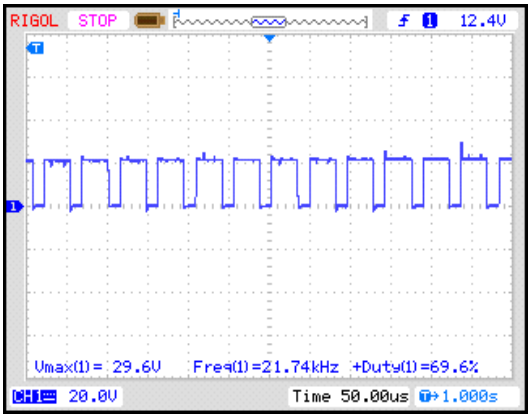

Figure 28. Comparitive Hardware and Simulink Results of Voltages Across Switch 2

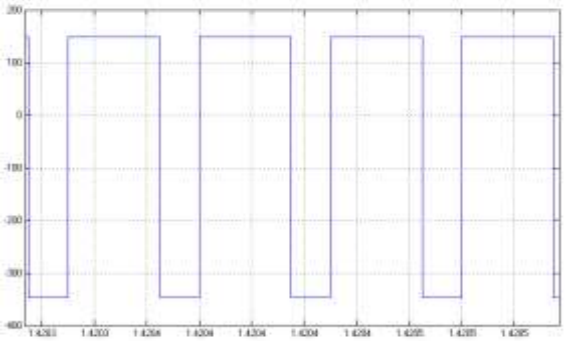

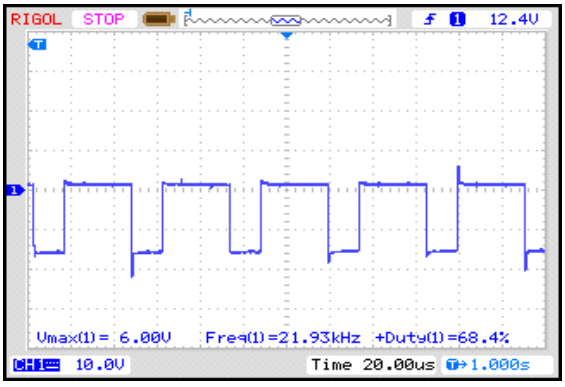

Figure 29. Simulink and Hardware Voltages Across D1

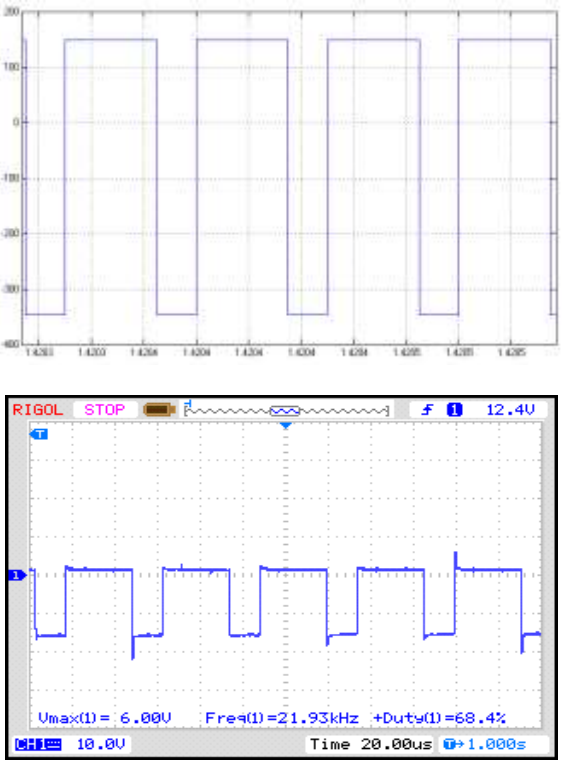

Figure 30. Simulink and Hardware Voltages Across D2

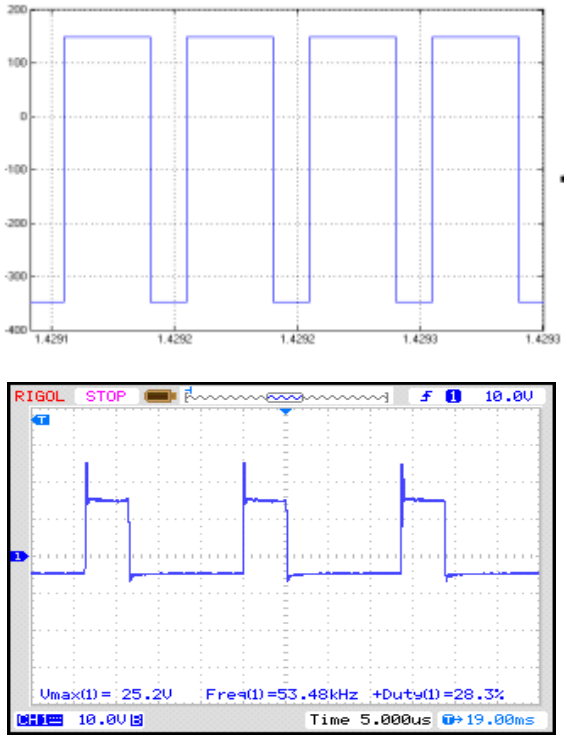

Figure 31. Simulink and Hardware Voltages Across L1 and L2

6. CONCLUSION

Due to increased consumption of electric power, demand for electrical generation always grows. To meet this requirement with non-polluting generation, renewable energy sources gains much importance these days. Out of which PV gives us an option to generate energy with low running cost with good efficiency during daylight. The output of the PV cell is low voltage DC and we need to step up this to high voltage. The output of PV is fed to an interleaved boost converter and then to an inverter. The DC output of PV is increased when low voltage DC is fed to interleaved boost converter. We used interleaved boost converter which cancels the ripples when compared to high ripple content in a normal boost converter. The output results show the reduction in ripple content when interleaved boost converter is used and the results were compared with normal boost converter. A simple prototype was developed to implement the above said model and its hardware results were also shown. This proves interleaved boost converter gives us good speed regulation with less ripple content with good efficiency.

REFERENCES

[1] Interleaving is Good for Boost Converters, Too, By Ron Crews and Kim Nielson, *Power Electronics Technology*, May 2008.

[2] Burak Akin, "*Comparison of conventional and interleaved PFC boost converters for fast and efficient charge of Li-ion batteries used in electrical cars"*, International Conference on Power and Energy Systems, vol. 13, pp. 499-504, 2012.

[3] Gustavo, A.L. Henn, R.N.A.L. Silva, Paulo P. Praca Luiz H.S.C. Baretto, and Demercil S. Oliveira, Jr. "Inerleaved boost converter with high voltage gain", *IEEE Trans. on Power Electrons*, vol. 25, no. 11, pp. 2753-2761, Nov. 2010.

[4] Jun Wen, Jin T, Smedley K, *"A new interleaved isolated boost converter for high power applications*", Applied Power Electronics Conference and Exposition, 2006. APEC '06. Twenty-First Annual IEEE, pp. 6 pp. 19-23 March 2006

[5] Giral, R.; Martinez-Salamero, L.; Leyva, R.; Maixe, J.; "Sliding-mode control of interleaved boost converters", Circuits and Systems I: Fundamental Theory and Applications, *IEEE* Transactions on, vol. 47, no. 9, pp. 1330-1339, Sep 2000

[6] Van der Broeck, H.; Tezcan, I.; *"1 KW Dual Interleaved Boost Converter for Low Voltage Applications*", Power Electronics and Motion Control Conference, 2006. IPEMC 2006. CES/IEEE 5th International, vol. 3, no. 1, pp. 1-5, 14-16 Aug. 2006

[7] Chen Chunliu; Wang Chenghua; Hong Feng; *"Research of an interleaved boost converter with four interleaved boost convert cells"*, Microelectronics & Electronics, 2009. PrimeAsia 2009. Asia Pacific Conference on Postgraduate Research, pp. 396-399, 19-21 Jan. 2009

[8] Rosas-Caro, J.C.; Ramirez, J.M.; Garcia-Vite, P.M.; *"Novel DC-DC Multilevel Boost Converter*", Power Electronics Specialists Conference, 2008. PESC 2008. IEEE, pp. 2146-2151, 15-19 June 2008

[9] Samosir, A.S.; Yatim, A.H.M.; "*Implementation of new control method based on dynamic evolution control with linear evolution path for boost dc-dc converter"*, Power and Energy Conference, 2008. PECon 2008. IEEE 2nd International, pp. 213-218, 1-3 Dec. 2008

[10] AN-1820 LM5032 Interleaved Boost Converter, Texas Instruments, Application Report SNVA335A–May 2008–Revised May 2013.

[11] R. Seyezhai, "Design, Simulation and Hardware Implementation of a Multi Device Interleaved Boost Converter for Fuel Cell Applications", *International Journal of Power Electronics and Drive System (IJPEDS)* Vol. 4, No. 3, pp. 314~320, September 2014.

[12] G. Seshagiri Rao, S. Raghu, N. Rajasekaran, "Design of Feedback Controller for Boost Converter Using Optimization Technique*", International Journal of Power Electronics and Drive System (IJPEDS)*, Vol. 3, No. 1, pp. 117~128, March 2013.

[13] R. Arulmurugan, N. Suthanthira Vanitha, "Optimal Design of DC to DC Boost Converter with Closed Loop Control PID Mechanism for High Voltage Photovoltaic Application*", International Journal of Power Electronics and Drive System (IJPEDS)* Vol. 2, No. 4, pp. 434~444, December 2012.

BIOGRAPHIES OF AUTHORS

Mr. A. Ramesh received his B. Tech in Electrical &Electronics Engineering and M.Tech in High Voltage Engineering from JNTU College of Engineering, Kakinada, Andhra Pradesh, India. He is pursuing Ph. D in Multilevel Inverter Technologies at K.L. University India. Currently he is working as Associate Professor in the Department of Electrical and Electronics Engineering, Aditya Engineering College, Surampalem, A.P. India. He is a life member of the Indian Society for Technical Education.

Dr. M. Siva Kumar was born in Amalapuram, India in 1971. He received bachelor's degree in Electrical & Electronics Engineering from JNTU College of Engineering, Kakinada and M.E and PhD degree in control systems from Andhra University College of Engineering, Visakhapatnam, in 2002 and 2010 respectively. His research interests include model order reduction, interval system analysis, design of PI/PID controllers for Interval systems, sliding mode control, Power system protection and control. Presently he is working as Professor & H.O.D of Electrical Engineering department, Gudlavalleru Engineering College, Gudlavalleru, A.P, India.

O. Chandra Sekhar received his B. Tech degree in Electrical & Electronics Engineering from JNTUH, India in 2005 and M. Tech with power Electronics and Electrical Drives from Vignan's Engineering College, Vadlamudi, India in 2008. He obtained his Ph. D. from J.N.T.U College of Engineering, Hyderabad in 2014. He has been with K.L. University, India as Professor. His Research interests are Power Electronics, Industrial Drives.